Journal of proteome research

ARTICLE

pubs.acs.org/jpr

Ookinete-Interacting Proteins on the Microvillar Surface are Partitioned into Detergent Resistant Membranes of *Anopheles gambiae* Midguts

Lindsay A. Parish,[†] David R. Colquhoun,[†,‡] Ceereena Ubaida Mohien,[†,‡] Alexey E. Lyashkov,[‡] David R. Graham,[‡] and Rhoel R. Dinglasan*[,†]

[†]W. Harry Feinstone Department of Molecular Microbiology & Immunology, Malaria Research Institute, Johns Hopkins Bloomberg School of Public Health, 615 North Wolfe Street, Baltimore, Maryland 21205, United States

[‡]Department of Molecular and Comparative Pathobiology, Johns Hopkins University School of Medicine, 733 North Broadway, Baltimore, Maryland 21205, United States

Supporting Information

ABSTRACT: Lipid raft microdomains, a component of detergent resistant membranes (DRMs), are routinely exploited by pathogens during host-cell entry. Multiple membrane-surface proteins mediate *Plasmodium* ookinete invasion of the *Anopheles* midgut, a critical step in the parasite life cycle that is successfully targeted by transmission-blocking vaccines (TBV). Given that lipid rafts are a common feature of host-pathogen interactions, we hypothesized that they promote the partitioning of midgut surface proteins and thus facilitate ookinete invasion. In support of this hypothesis, we found that five of the characterized *Anopheles* TBV candidates, including the leading *Anopheles* TBV candidate, AgAPN1, are present in *Anopheles gambiae* DRMs. Therefore, to extend the repertoire of putative midgut ligands that can be targeted by TBVs, we analyzed midgut DRMs by tandem mass spectrometry. We identified 1452 proteins including several markers of DRMs. Since glycosylphosphotidyl inositol (GPI)-anchored proteins partition to DRMs, we characterized the GPI subproteome of *An. gambiae* midgut brush-border microvilli and found that 96.9% of the proteins identified in the GPI-anchored fractions were also present in DRMs. Our study vastly expands the number of candidate malarial TBV targets for subsequent analysis by the broader community and provides an inferred role for midgut plasmalemma microdomains in ookinete cell invasion.

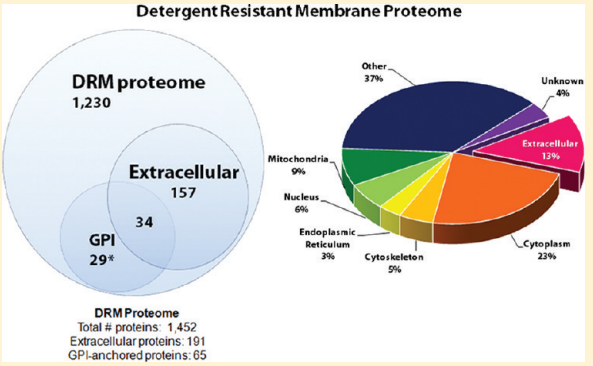

KEYWORDS: *Plasmodium*, ookinete, *Anopheles gambiae*, midgut, transmission blocking vaccine, detergent resistant membranes, lipid rafts, malaria

INTRODUCTION

Malaria remains a significant cause of morbidity and mortality across the globe despite efforts to control the disease. The spread of drug resistant parasites and insecticide resistant mosquitoes highlight the need for innovative strategies that can eventually lead to the elimination of malaria. One approach that has recently regained momentum is the concept of transmission-blocking vaccines (TBV), which interrupt the development of *Plasmodium* parasites, the causative agents of malaria, within the *Anopheles* mosquito.[1] In order to be transmitted to a human host, parasites must travel from the mosquito midgut lumen to the salivary glands. Inside the midgut lumen, *Plasmodium* gametocytes that are ingested with a blood meal transform into invasive ookinetes, which then interact with the midgut surface prior to active cell invasion. Following cell traversal to the basal side of the midgut cell, the ookinete develops into an oocyst, which ultimately releases thousands of sporozoites that invade the mosquito salivary glands. Once in the salivary glands, these sporozoites are now primed and ready to infect a vertebrate host once the mosquito takes its next blood meal. Ookinete invasion of the midgut represents the first invasion bottleneck in the parasite's complex life cycle within the mosquito, offering a unique opportunity to interrupt malaria transmission.[1] Therefore, defining the molecular interactions between the ookinete and the lumenal surface of the *Anopheles* midgut is crucial to understanding the biology of transmission and for the development of novel transmission-blocking interventions.

Previous studies have proposed that ookinetes interact with multiple glycans and glycoproteins on the apical (lumenal) surface of the midgut, (reviewed in refs 2 and 3), and these glycoconjugates represent a set of potential targets for mosquito-based malaria TBVs (Table 1). As multiple midgut surface macromolecules appear to be necessary for midgut invasion by

Received: July 4, 2011
Published: September 09, 2011

Table 1. Known Ookinete-Interacting Proteins Identified in DRM Fractions[a]

accession no.	annotation	evidence for role of molecule in *Plasmodium* development	reference
AGAP004809	GPI-anchored Aminopeptidase N	Anti-AgAPN1antibodies inhibited both P. *falciparum* (70−80%) and *P. berghei* (70−80%) oocyst development	11
AGAP003790	Annexin-like	Anti-ANXB9 antibodies inhibited of *P. berghei* (30−38%) oocyst development	12
AGAP003721	Annexin-like	Anti-ANXB10B antibodies inhibited *P. berghei* (36−40%) oocyst development	12
AGAP003722[b]	Annexin-like	Anti-ANXB10C antibodies inhibited 28.2−43.7% of *P. berghei* development in the midgut	12
AGAP006209	Carboxypeptidase B	Antibodies against CpbAg1 inhibited both *P. falciparum* and *P. berghei* development	13
AGAP010133	Scavenger Receptor, Croquemort Homologue	Knock-down of *SCRBQ2* results in a 62.5% inhibition of *P. berghei* oocyst formation	14

[a] *An. albimanus* calreticulin (AaCrt) has been shown to localize to the apical surface of *An. albimamus* midguts and to interact with a recombinant form of the abundant *P. vivax* ookinete surface protein, Pvs25.[15] The *An. gambiae* homologue of AaCrt, AGAP004212, was present in DRMs but was not included in Table 1, since to date, there is no direct evidence by either RNAi knock-down or the use of anti-AaCrt antibodies demonstrating the involvement of *Anopheles* midgut surface expressed calreticulin in *Plasmodium* invasion and establishment in the mosquito. [b] Only known ookinete-interacting protein not detected in the DRM proteome.

Plasmodium ookinetes, a model is needed to explain mechanistically how ookinetes coordinate multiple protein−protein and protein−glycan interactions with the apical surface of the midgut at a defined point of cell entry.

One idea is based on the hypothesis that host cell membrane microdomains mediate surface protein organization and that pathogens utilize these sites for adhesion complex formation and subsequent attachment and invasion.[4] Lipid microdomains commonly referred to as "lipid rafts", exhibit dynamic lateral movement on the cell surface and are enriched in proteins that facilitate various cellular functions including signal transduction, cell adhesion, and vesicle trafficking (reviewed in ref 5). Rafts compartmentalize these cellular processes by partitioning, both temporally and spatially, specific proteins into distinct phases of the plasma membrane. Biochemically, lipid rafts are characterized by a high density of cholesterol and sphingolipids. The tight packing of sterols between the saturated sphingolipid acyl chains forms a lipid ordered phase within the plasma membrane.[6] This intrinsic property allows rafts to be resistant to solubilization by nonionic detergents such as Triton X-100 at 4 °C. Although a pure fraction of lipid rafts cannot be isolated, a detergent resistant membrane (DRM) fraction, which is enriched in lipid rafts and associated proteins, can be separated from other membrane proteins and lipids through detergent extraction followed by density gradient centrifugation.[7,8]

A variety of pathogens induce the fusion of multiple rafts to create large clusters of host receptors in a concentrated region of the membrane.[9] This allows for the enhancement of multivalent protein−protein[9] and protein−glycan[10] interactions between the pathogen and the host cell that are necessary for attachment and invasion to occur. It is unknown if *Plasmodium* parasites engage *Anopheles* midgut lipid rafts in a similar fashion. However, given that exploitation of host lipid rafts by pathogens appears to be a common theme, we hypothesized that during the multistep process of midgut invasion, *Plasmodium* ookinetes promote the formation of an adhesion complex on the surface of the *Anopheles* midgut through the subversion of apical microvillar lipid rafts. The underlying premise is that midgut invasion requires the concentration of a diverse set of microvillar glycans and glycoproteins that act cooperatively as adhesion and invasion ligands for the ookinete. To date, at least six midgut surface molecules[11−15] have been shown to mediate parasite−vector host interactions and consequently have been proposed as potent candidate TBV targets (Table 1). Therefore, a reasonable test of our hypothesis would be to determine if these targets are enriched in DRMs. If some or all of these targets are enriched in DRMs, then it is possible that several other uncharacterized molecules may prove to be important mediators for ookinete invasion and, as such, the handful of proteins in Table 1 represents only a fraction of the total number of potential TBV targets, and that other glycoproteins that are resident or enriched in midgut DRMs, represent the untapped pool of vaccine candidates. We therefore used a proteomics approach to characterize the broad repertoire of lumenal glycoproteins that reside in an enriched sample of apical midgut surface DRMs. Using an extensive fractionation and informatics strategy, we were able to identify over 1400 proteins that will hopefully help us glean new insights into the mechanism(s) of *Plasmodium* ookinete invasion of the midgut and provide an extensive catalog of potentially new TBV targets and protein identities for the broader malaria and vector biology communities.

MATERIALS AND METHODS

Preparation of *An. gambiae* Midguts for Analysis

For each DRM preparation, approximately 1000 midguts were dissected and 1 mL of a solution of 1% Triton X-100 in TKM buffer (50 mM Tris-HCl, pH 8, 25 mM KCl, 5 mM $MgCl_2$, 1 mM EDTA) was added to the sample. The sample was then homogenized on ice with a Dounce homogenizer for 45 min. Following homogenization, the sample was incubated on ice for one hour. Then the midgut lysate was mixed with an equal volume of 80% sucrose and layered in the bottom of an ultra centrifuge tube. The sample was incubated on ice for one hour in the centrifuge tube. Next, 6 mL of 38% sucrose were layered slowly on top of the previous layer, followed by layering 4 mL of 5% sucrose. The sample was then subjected to ultracentrifugation for 18 h at 4 °C at 100 000× *g* with no brake. After ultracentrifugation, 1 mL fractions were collected from the top of the sucrose gradient. The resulting fractions were precipitated in 15% w/v trichloroacetic acid overnight at 4 °C and resuspended in 100 μL 1× ProteaseMax (Promega) in 55 mM NH_4HCO_3.

Cholesterol Quantification

Cholesterol detection and quantification from *An. gambiae* midgut extracts was performed by using the Amplex Red cholesterol assay kit (Invitrogen) according to the manufacturer's instructions. Briefly, using a cholesterol standard provided with the kit,

we measured the levels of cholesterol in the midgut extracts, reported as nanograms of cholesterol per microgram of protein.

Brush Border Microvilli Vesicles (BBMV) Preparations

Approximately 300−400 female mosquito midguts were transferred to 200 μL of microvilli buffer (50 mM D-mannitol, 20 mM Tris-HCl, pH 7.4, protease inhibitor cocktail (Sigma), 1 mM PMSF, 3 mM imidazole-HCl (Sigma). The midguts were then homogenized on ice using 30 strokes of a Dounce homogenizer. The sample was then brought up to 10 mL in microvilli buffer and 0.05 g of $MgCl_2$ were added to sample and mixed by vortexing. After a 20 min incubation on ice, the sample was centrifuged at 805× *g* for 10 min at 4 °C. The supernatant was saved and the pellet was resuspended again in 10 mL of microvilli buffer and extracted two more times as described above. The supernatants from all extractions were transferred to a high speed centrifuge tube and subjected to ultracentrifugation at 30 000× *g* for 1 h at 4 °C. The resulting supernatant was discarded and the pellet was resuspended in a final volume of PBS equivalent to 1 μL PBS/midgut. Protein quantification of all protein samples for each biological replicate was performed using a BCA Protein Assay Kit (Pierce, Rockford IL) according to the manufacturer's instructions.

Preparation of GPI-Anchored Protein Enriched Fractions

The three biological replicate BBMV samples prepared from *An. gambiae* midguts were treated with 1 Unit of *Bacillus cereus* glycosylphosphotidyl inositol-specific phospholipase C (PI-PLC) (Sigma) at room temperature overnight. The sample was then centrifuged at 17 000× *g* for 10 min and the supernatant containing glycosylphosphatidylinositol (GPI) anchored proteins was collected.

Trypsin Digestion

For analysis of the DRM fractions, 10 μg of protein from each fraction (fraction 4, 5, and 6) was dried by vacuum centrifugation and the sample was then resuspended in 20 μL of 20 mM NH_4HCO_3 (Sigma). We added 1 μL of 50 mM dithiothreitol (DTT) (Invitrogen) to the sample prior to incubation for 15 min at 60 °C. We then added 5 μL of 22 mM iodoacetamide (Sigma) to the sample followed by incubation for 25 min at room temperature in the dark. Proteomics grade trypsin (Sigma, cat. # T6567) was added to sample (1:50) and incubated at 37 °C for overnight. For GPI-anchored proteins samples, an in-gel digestion protocol was used. Approximately 10 μg of an enriched GPI-anchored protein sample was run on a NuPAGE 4−12% gel (Invitrogen), using 1× MES SDS NuPAGE running buffer (Invitrogen) for one hour at 200 V. Following overnight staining with Sypro Ruby (Invitrogen, Carlsbad, CA), and imaging on a 9210 Typhoon scanner (GE) (PMT of 500 V and 25 μM resolution), the entire lane was cut into 11 gel fragments. Gel pieces were dehydrated for 5 min in 200 μL of acetonitrile: 50 mM NH_4HCO_3. Gel pieces were dried in a vacuum centrifuge and then rehydrated in 100 μL of 25 mM DTT in 50 mM NH_4HCO_3 and incubated for 20 min at 56 °C. The supernatant was discarded and 100 μL of 55 mM iodoacetamide in 50 mM NH_4HCO_3 was added to gel pieces and incubated at room temperature in the dark. The supernatant was discarded and gel pieces were washed in 1 mL of Milli-Q water. Next, the supernatant was discarded and gel fragments were dehydrated as described above. Gel pieces were rehydrated in 75 μL of 0.01% ProteaseMax containing 2 ng/μL trypsin. Gel pieces were incubated at 37 °C for 3 h. Following a brief centrifugation, the supernatant was collected, dried, and resuspended in 2% acetonitrile, 0.1% TFA for LC−MS/MS analysis.

Peptide Fractionation

For each DRM preparation, the digested, dried peptides were separated using an Agilent 3100 OFFgel fractionator (Agilent, Santa Clara, CA). Samples were loaded onto a rehydrated 24 cm pH 3−10 IEF strip (GE Healthcare, Piscataway, NJ) in 0.5% ampholytes in water. The peptides were separated for 50 kVhrs at 20 °C, with maximum values of 4500 V, 50 μA and 200 mW. Paper wicks were exchanged as per standard protocols. Upon focusing, samples were removed from the sample wells, acidified with formic acid, and dried using a vacuum centrifuge. Peptides were resuspended in 8 μL 2% acetonitrile, 0.1% (*w*/*v*) trifluoroacetic acid for LC−MS/MS analysis.

LC−MS/MS

Biological replicates were analyzed independently as follows. The entire 8 μL sample was injected onto an Agilent LC−MS system comprised of a 1200 LC system coupled to a 6520 Q-TOF via an HPLC Chip Cube interface. The sample was trapped and analyzed using an Agilent large capacity HPLC chip (160 nL, 300 Å C18 trap with a 150 mm, 300 Å C18 analytical column). Peptides were loaded onto the chip using 97% solvent A (0.1% formic acid in water) and 3% solvent B (0.1% formic acid in 90% acetonitrile) at a flow rate of 3 μL/min. Elution of peptides from the analytical column was done using a stepped gradient starting at 97% A at 300 nL/min. A linear gradient from 10 to 40% solvent B was applied from 2 to 80 min. The gradient was then stepped to 99% B and back to 97% A at 90 min. A 5-min re-equilibration step was applied to the end of each run. Column flow throughout the run was analyzed by the 6520 Q-TOF in 2 GHz data dependent (autoMS2) mode with internal reference masses (*m*/*z* 391.28 and 1222.99). Precursor MS spectra were acquired from *m*/*z* 300 to 1600 and the top 4 peaks (+2, +3 and > +3 charge states, intensity >1000) were selected for MS/MS analysis. Product scans were acquired from *m*/*z* 50 to 1600 at a scan rate of 1.7/second. A medium isolation width (∼4 amu) was used, and a collision energy of slope 3.9 V/100 Da with a 2.9 V offset was applied for fragmentation. A dynamic exclusion list was applied, with precursors excluded of 0.13 min after one MS/MS spectrum was acquired.

Data Analysis

The data acquired from Agilent Mass Hunter 2.3.0 was searched against the *Anopheles gambiae* proteome fasta database (*An. gambiae* P6 release, VB-2011−04) downloaded from VectorBase (http://www.vectorbase.org/GetData/Downloads/). The data was first searched with multiple search engines (Mascot,[17] OMSSA[18] and X!Tandem[19] with native scoring) with the following parameters: carbamidomethylation and oxidized methionine set as variable modification, mass tolerances on precursor and fragment ions set as 30 and 20 ppm respectively and missed cleavage as 1. We then combined these search results by a meta-search methodology. MS raw files were converted to mzXML format using Trapper (ISB) and searched by PepArML which uses an unsupervised, model-free, combining framework.[20] All of the computed search results were combined by the PepArML result combiner, employing a random forest machine learning technique, based on the Weka software package,[21] to generate a consensus set of peptide-spectrum matches. Multiple decoy searches were also used to estimate the statistical significance of the final resulting protein identifications. Two decoy database

replicates were selected to increase the precision of the false discovery rate (FDR) estimation process. Proteins with at least 2 peptides at <1% FDR and peptide length >5 amino acids were stored for subsequent query and retrieval by Maspectras 2.[22] Identifications that passed these criteria were then grouped according to shared peptides (MS-evidence grouping, to eliminate isoforms, splice variants and fragments which share peptides) and the representative protein of the group was considered as a unique protein identification. The data analysis pipeline meets all MIAPE standards[22] and has been uploaded to Tranche (https://proteomecommons.org/tranche). The bioinformatics methodology was designed to obtain a maximum of true positives while minimizing false positives and false negatives. Several publications have detailed the need for several parallel search engine processes.[23−25] As such, we used a meta-search strategy based on the PepArML result combiner.

Our use of multiple search engines (Mascot, OMSSA, and X! Tandem) within the PepArML meta-search engine platform, substantially increased the number of proteins identified for each of the three representative DRM preparations (Figure S1, Supporting Information) to 1452 proteins at a stringent cutoff of <1% FDR (Table S1, Supporting Information). As to the rate of peptides to spectra, PepArML framework identified 12 040 peptides for 167 045 spectra. For the GPI subproteome, the peptide assignments for GPI proteins are 393 peptides for 5392 spectra using PepArML.

The manual curation of the 1452 identified DRM proteins was performed using the conserved domains as predicted by VectorBase (AgamP6, VB-2011−04), InterPro, Pfam, UniProt, and BLAST searching using the nonredundant protein sequences database on NCBI. If multiple different conserved domains were listed in a single protein, the larger conserved domain was used to classify that protein. To predict which proteins are extracellular and exposed to the midgut lumen, only proteins which had a signal sequence (with the exception of galectins, annexins ANXB10B and ANXB9, and stomatin) and were not predicted to be intracellular based on sequence homology and annotation were counted.

Agglomerative Hierarchical Clustering

Agglomerative hierarchical clustering (AHC) was performed by normalizing the spectral counts for each protein observed obtained from Maspectras to the number of total spectra observed for that group, and expressed as a percentage, using Microsoft Excel for Windows 2007. AHC was calculated using XLstat specifying Euclidean distance by dissimilarity and using Ward's method as the agglomeration method (Table S2, Supporting Information).

Production of anti-AgEcad Antibodies

The AgEcad primers for AGAP007203, (AgEcad Forward, 5′-CAC CAT GGT TGG TAC GCC GGT ACT GCG CGT-3′, AgEcad Reverse, 5′-CTG CTC CAG CAG GAA TGT ATT TTT CGA-3′) were used to clone a 779 base pair fragment of *AgEcad* into the TOPO vector pBAD202D (Invitrogen) and expressed in *E. coli*. AgEcad is a homologue of DE-cadherin/shotgun in *Drosophila*, which is involved in adherens junction integrity between adjacent midgut epithelial cells and is distributed primarily along the basolateral domain of polarized cells.[26,27] The resulting recombinant his-tagged protein was purified using Ni-agarose beads (Qiagen). Rabbit polyclonal antiserum was generated against the purified recombinant protein (Washington Biotechnology, Inc.) and recognized a single protein band of the expected size.

Immunoblot Analysis

Approximately 20 μg of protein from each of the sucrose fractions were run in each lane of a 4−12% Bis-Tris Invitrogen gel (using conditions described above) and transferred to a nitrocellulose membrane for one hour at 100 V at 4 °C. Immunoblots were probed with either1:200 α-AgAPN1 (11) or 1:50 α-AgEcad. Primary antibodies were detected by α-rabbit secondary antibodies CW 800 (LI-COR) and detected on an Odyssey infrared imaging system. Quantification of the APN1 bands was performed using the LI-COR Odyssey 3.0 application software.

RESULTS AND DISCUSSION

To test our hypothesis, we isolated *An. gambiae* midgut DRM fractions from 1,000 *An. gambiae* sugar-fed midguts for each of our three biological replicate DRM preparations. In this study, we chose to use sugar-fed midguts as opposed to blood-fed midguts for the following reasons: (a) two previous studies have shown that several midgut surface proteins, including AgAPN1 (AGAP004809, Table 1), are expressed on the surface of sugar-fed midguts,[11,28] and (b) by analyzing sugar-fed midguts, we avoided gross contamination of our midgut DRM sample with human blood and serum proteins, which would complicate the analysis. Very little is known about the protein expression profile of the panoply of genes that have been shown by functional genomics analyses to be upregulated in response to ookinete invasion of the midgut.[29,30] Therefore, given what is known about AgAPN1, we also sought to determine if these proteins are present in sugar-fed midguts.

After ultracentrifugation of the Triton X-100 midgut lysate, we observed that lipid rafts are indeed visible at the interface between the 5 and 38% sucrose layers, represented as fractions 4, 5, and 6 (Figure 1a−c and Figure S1, Supporting Information). Three independent DRM preparations were isolated for analysis by tandem mass spectrometry. GPI-anchored proteins, which are associated with DRMs are frequently used as markers of DRMs to confirm DRM enrichment.[4,5] To indirectly confirm the presence of GPI-anchored proteins, immunoblots of fractions and the pellet from the sucrose gradient were probed with antibodies that recognized *An. gambiae* amino peptidase N, AgAPN1, a microvillar GPI-anchored glycoprotein, which is currently the leading mosquito based TBV target (Figure 1d).[11] As expected, immunoblots probed with specific antisera to AgAPN1 recognized the predicted M_r = ∼125 kDa and protein double band at M_r = ∼60 kDa.[11] These data indicate that AgAPN1 is present across all fractions, but is particularly concentrated in the DRMs (fractions 4, 5, and 6) and the pellet (Figure 1d). In addition, specific antibodies were raised against a recombinant fragment of the *An. gambiae* E-cadherin homologue (AgEcad, AGAP007203) of the adherens-junction DE-cadherin/shg in *Drosophila*.[26,27] This protein was selected as a marker for non-DRM proteins and used to demonstrate the differential separation of DRM-associated proteins through sucrose gradient fractionation. Immunoblots probed with AgEcad specific antisera revealed that AgEcad was detectable only in the pellet fraction (Figure 1e).

Detection and Quantification of Cholesterol in *An. gambiae* Midguts

Cholesterol, which is enriched in lipid rafts, is found in the membranes of almost all eukaryotes. Insects such as *An. gambiae*, do not synthesize cholesterol *de novo* as they lack the genes for key enzymes necessary for cholesterol biosynthesis.[31] However, *Aedes aegypti* larvae are capable of synthesizing cholesterol from

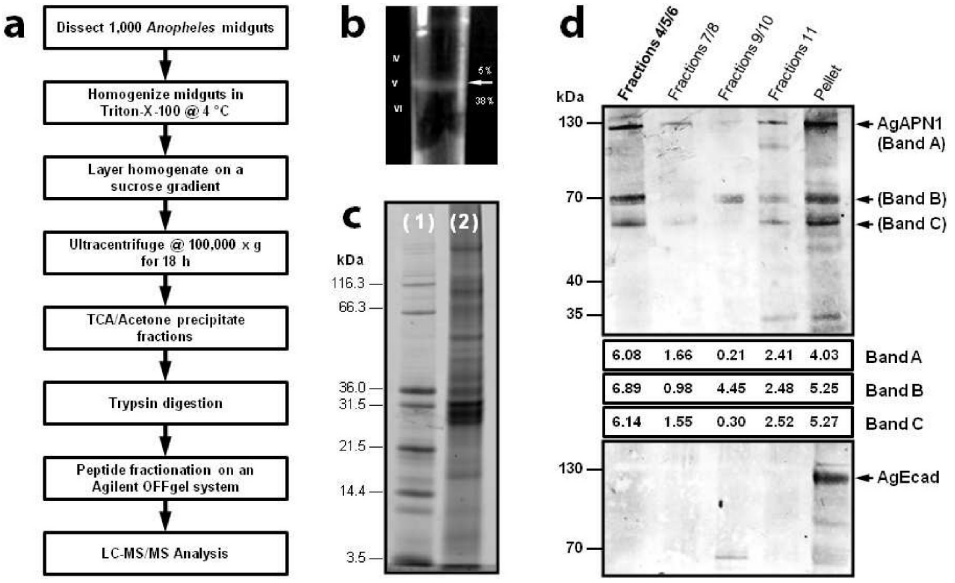

Figure 1. Isolation and purification of *Anopheles gambiae* adult midgut Detergent Resistant Membranes (DRMs). (a) Experimental work-flowchart for the isolation of DRM fractions of *An. gambiae* midguts. For each biological replicate, approximately 1000 mosquitoes midguts were dissected then homogenized in 4 °C with 1% Triton X-100. Samples were layered on a sucrose gradient, centrifuged at 100 000× *g* for 18 h. Fractions were TCA/acetone precipitated, digested with trypsin, and analyzed by LC−MS/MS. (b) Photograph of the DRM layer in sucrose gradient following ultracentrifugation. Regions IV, V, VI correspond to fractions 4, 5, and 6. (c) SDS-PAGE SYPRO Ruby stained gel. Lane (1), molecular weight markers (kDa), Lane (2), 5 μg/well of fractions 4, 5, and 6 (DRM fractions). (d) Immunoblot analysis of *An. gambiae* adult midgut DRMs shows an enrichment of AgAPN1 in DRM Fractions. Following sucrose density gradient ultracentrifugation, 11 × 1-mL fractions and a pellet were collected. Equal amounts (20 μg) were probed for AgAPN1 and AgEcad with the respective antibodies. Fractions 4/5/6 (bold) represent the pooled DRM fraction (see text for details). Near infrared fluorescence quantification expressed as integrated intensity as measured by the Odyssey System (LI-COR) for each of the three respective AgAPN1 protein bands (Bands A, B and C) present across different fractions is indicated in boxed rows. The quantification data suggest AgAPN1 is more concentrated in fraction 4/5/6 (lane 1) and pellet as compared to other fractions (fractions 7 and 8; fractions 9 and 10; and fraction 11).

other dietary sterol precursors.[32,33] Additionally, a sterol carrier protein-2 homologue was found in *A. aegypti* and shown to facilitate cholesterol uptake in cultured cells.[34,35] To our knowledge, there is no published report confirming the presence of cholesterol in female adult *An. gambiae* midguts. Since cholesterol is a key component of DRMs, we analyzed fractions from the sucrose gradient to determine if cholesterol is present and enriched in the DRM fractions (fractions 4, 5, and 6). Samples of the midgut Triton X-100 lysate before ultracentrifugation were used to determine the total amount of cholesterol. We estimated the presence of approximately 12.17 ng cholesterol/μg of protein in our total midgut lysate from two biological replicate samples. Next, to confirm enrichment of cholesterol in the putative DRM fraction, samples from fractions 4, 5, and 6 postultracentrifugation were analyzed. These putative DRM fractions had an averaged 4.41 fold increase in cholesterol/μg protein as compared to the total midgut lysate as determined from two biological replicate samples. These data complement our visualization of DRMs after ultracentrifugation (Figure 1b) and suggest that fractions 4, 5, and 6 are enriched in DRMs. It is important to note that the assay used cannot distinguish between cholesterol and cholesterol esters.

Proteomic Analysis and Classification of *An. gambiae* Midgut Detergent Resistant Membrane-Associated Proteins

To capture the midgut DRM proteome we used a complex sample fractionation strategy coupled with thorough mass spectrometric analyses. After DRM enrichment, replicate samples were digested using standard protocols and then heavily separated by peptide-level isoelectric focusing into 24 fractions followed by LC−MS/MS. This approach was used to increase the probability of achieving greater coverage of proteins and allowed us to detect more low-abundant proteins. The advantage of such an approach is that with a greater coverage, a more detailed atlas of the DRM proteome can be generated.

We used a combination of multiple search engines and machine learning recombination to maximize the number of assigned spectra and minimize the false discovery rates. Furthermore, to minimize any protein redundancy in our protein assignments, an advanced clustering method was used (see Methods). Using this advance informatics workflow, we identified 1452 proteins using a highly stringent cutoff of <1% FDR (false discovery rate) (Table S1, Supporting Information). Given the number of spectra assigned, we were able to use agglomerative hierarchical clustering (AHC) analysis to determine the degree of variability between the three biological DRM preps (Table S2, Supporting Information). This method takes into consideration distance and relations of all of the factors, and is a much more robust method of determining reproducibility than Venn diagrams showing common proteins. This analysis showed a striking degree of similarity (>80%) between the replicates that were the greatest distance from another. Given the potential degree of variability in fraction collection and preparation and the random nature of spectral acquisition in data-dependent MS/MS studies, this degree of similarity represented excellent reproducibility between biological replicates and permitted the pooling of the data sets.

We manually curated all of the 1452 identified proteins to gain molecular insight for the proteins identified using our approach (Figure 2 and Table S1, Supporting Information). These 1452

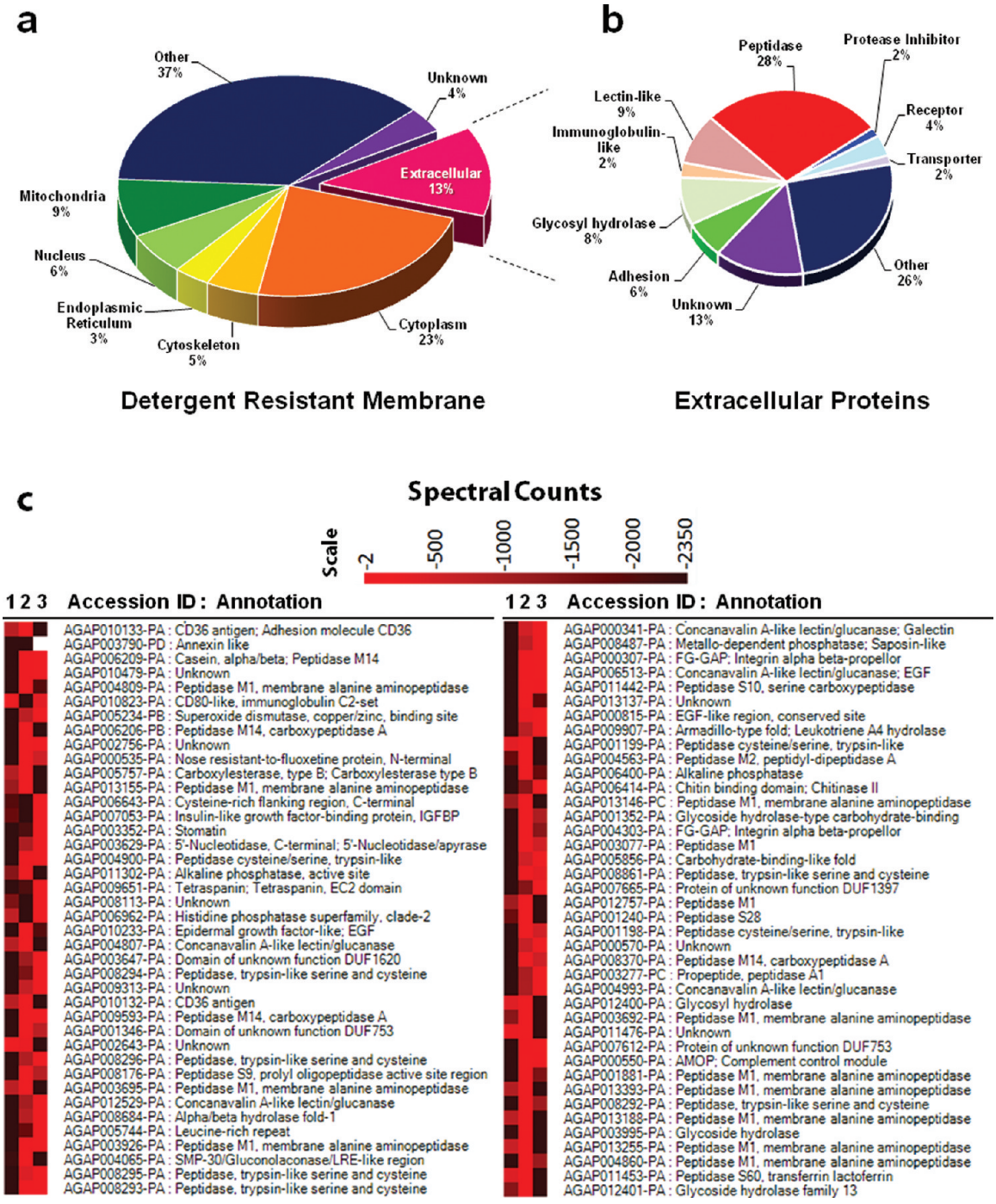

Figure 2. Characterization of the *An. gambiae* adult midgut DRM proteome. (a) Distribution of the total DRM proteins into categories based on intracellular location (N = 1,452) (see text and Table S1, Supporting Information, for details). (b) Distribution of the predicted extracellular DRM proteins into categories based on function (N = 191). (c) Spectral heat map representing a subset of extracellular proteins (N = 80) that were identified across the three biological DRM replicates (FDR < 1%), with the exception of AGAP003790. Included in this map are four out of the six the current transmission-blocking vaccine candidates listed in Table 1, as well as canonical lipid raft markers (see text and Table S4, Supporting Information, for details). Each row shows the row-normalized number of spectral identifications for each protein from each run (see scale bar). Normalization was carried out as described previously.[16]

proteins were annotated functionally according to conserved domains as predicted by VectorBase (VB-2011−04), InterPro, UniProt, and BLAST searching using the nonredundant protein sequences database on NCBI. The identified proteins were then assigned to various categories based on their predicted cellular localization (Figure 2a). Bioinformatics analysis predicted that a considerable number of these proteins are likely to be cytoplasmic (23.1%) and cytoskeletal (5%). The presence of these proteins has been previously reported from biochemical and proteomic analyses of DRM preparations from many different

dx.doi.org/10.1021/pr2006268 |*J. Proteome Res.* 2011, 10, 5150–5162

cell types.[7,8] Components of the cytoskeleton have also been demonstrated to associate with DRMs *in situ*[36] and that the presence of these proteins is not surprising given the dynamic interactions occurring between lipid rafts and the cytoskeleton and cytoskeleton associated proteins. Previous analyses of an enrichment of midgut brush border microvilli (BBMV) membranes, which encompasses the same apical membrane face represented by our DRM fractions, also identified cytoplasmic proteins and cytoskeletal proteins.[37−39] At present it remains unclear which specific cytosolic proteins are mechanistically associated with DRMs and which are simply detergent-resistant contaminants. However, we noted that common DRM-associated proteins such as stomatin,[39] galectin-4 like proteins,[40] annexin-2,[41] alkaline phosphatase,[42] and protein 14-3-3[43] were all detected in our midgut DRM fractions. Also, proteins such as AgMuc1 (AGAP001192) and AgDuox (AGAP009978) were not detected in the DRM fractions illustrating that as expected not all midgut surface proteins are present in the DRM fractions.

To estimate the number of midgut DRM proteins that are potentially surface-associated, the amino acid sequences of all 1452 proteins were analyzed for the presence of a secretory signal sequence by SignalP (Table S1, Supporting Information). Many surface-associated proteins contain a signal sequence, which allows proteins to enter the secretory pathway and be trafficked to the plasma membrane. Of the 1452 proteins, 280 had a putative N-terminal signal sequence (Table S1, Supporting Information). However, not all surface-associated proteins contain a canonical signal sequence. Galectins, annexins, and stomatin were detected in our DRM fractions and categorized as extracellular proteins despite the lack of a signal sequence since these proteins are frequently surface-associated proteins in other organisms.[44,45] Furthermore, not all proteins with a signal sequence are surface-associated; thus, based on sequence homology and evidence in the literature, 89 intracellular proteins, which had a predicted signal sequence, were excluded from the extracellular DRM protein list. Altogether, a total of 191 DRM-associated proteins (FDR < 1%) were predicted to be extracellular and exposed to the midgut lumen (Table S2, Supporting Information). These 191 proteins were further classified according to predicted functional domains (Figure 2b). A heat map representing the spectral assignment for each extracellular protein for every DRM preparation is provided; demonstrating reproducible protein identifications across independent preparations for a majority of the proteins (Figure S3, Supporting Information). These findings are particularly relevant to our effort to identify midgut surface molecules as potential TBV candidate antigens. Mosquito TBVs based on midgut surface proteins, rely on the ability of antibodies to bind their target on the lumenal surface of the midgut epithelium subsequently following ingestion by a mosquito that took its bloodmeal from an immunized vertebrate host. To date, only six proteins have been studied as candidate TBV antigens (Table 1), by virtue of their knockdown by RNAi or direct targeting by antibodies. A heat map, highlighting the currently recognized TBV candidate antigens, as well as a subset of canonical lipid raft protein markers and potential TBV targets are shown in Figure 2c. From this analysis alone, the number of novel, putative vaccine targets has increased 27-fold.

Of the 191 predicted extracellular DRM-associated proteins, the common classes of proteins included: peptidases (27.7%), glycosyl hydrolases (8.4%), protease inhibitors (1.6%), lectins (8.9%), proteins involved in cell adhesion (6.3%), receptors (3.7%), proteins of unknown function (13.6%), transporters (1.6%), proteins containing an immunoglobulin-like domain (2.6%) and proteins classified as "other" which did not fall into any other category (25.1%) (Figure 2b and Table S3, Supporting Information). Previous studies have reported that DRM fractions from BBMVs are enriched in brush border enzymes.[42] These results are consistent with our findings, in which peptidases, both soluble and membrane bound, comprised 27.7% of the total predicted extracellular midgut DRM-associated proteins. The most common peptidases were trypsin-like and M1 membrane alanyl aminopeptidases such as AgAPN1 (Table S2, Supporting Information). A second group of enzymes detected in the DRM fractions are glycosyl hydrolases. These enzymes, which catalyze the release of glycans via hydrolysis of glycosidic bonds, have been reported to be present on the surface of cells[46] and adult mosquito midgut BBMVs,[11] as well as secreted into the lumen of the mosquito midgut during blood digestion.[47] Also, protease inhibitors, including Serpin-4 (AGAP009670), were detected in the DRM fractions. Serpins belong to a large family of serine protease inhibitors that regulate mosquito innate immune functions.[48] Lectins, a class of proteins that bind to specific glycans, were also detected in the DRM fractions and included five galectins and seven peritrophins. Galectins are a family of lectins that have affinity for β-galactosides, and some members of this family, such as galectin-4, have been shown to stabilize lipid rafts by forming a lattice-like network of galectin-glycan interactions.[40] In addition, peritrophins, which are proteins with chitin-binding domains and are associated with the peritrophic matrix (PM),[49] were detected in our DRM fractions despite the fact that our preparations used sugar-fed midguts that lack a peritrophic matrix. However, this observation is consistent with the report that PM proteins are synthesized and stored in secretory vesicles just beneath the apical plasma membrane before ingestion of a blood meal; thus, their proteomic detection in sugar-fed midguts is expected.[50] Moreover, DRMs and DRM-associated proteins have been shown to mediate secretory vesicle exocytosis and are hypothesized to cooperatively tether secretory vesicles and granules to "active zones" in the plasma membrane for rapid release.[51] Proteins categorized as adhesins included cadherin-like proteins, integrins, CD36 scavenger receptor homologues, and proteins containing a laminin domain. Integrins belong to a family of proteins that function to connect components of the extracellular matrix/glycocalyx to the cell cytoskeleton and play roles in cell−cell adhesion and signal transduction.[52] While many integrins are associated with the basal lamina, there are reports of integrins being associated with DRMs on the apical membrane.[53] Proteins categorized as receptors included two mannose-6-phophate receptors, an insulin-like growth factor binding protein, and a low-density lipoprotein receptor. Lastly, among the proteins of unknown function, AGAP000570 was previously reported as the most abundant protein in the *An. gambiae* PM proteome.[49] However, it is hypothesized that midgut microvilli are closely intercalated with the developing PM fibrils, which may implicate AGAP000570 as a tethering anchor for the PM. Thus, its inclusion in the PM proteome may be artificial, resulting from the dissection of the PM from the midgut epithelium during sample preparation.[49]

Immunoglobulin-like Proteins

A total of 29 proteins containing at least one immunoglobulin-like domain were detected in the DRM fractions (Table 2). Of the 29 immunoglobulin domain-containing proteins, 20.7% contained a signal sequence and therefore are potential secreted

Table 2. Midgut Detergent Resistant Membrane Proteins Containing an Immunoglobulin-like Domain

protein	conserved immunoglobulin-like domain	signal P	TMD
AGAP000550[a]	Ig E-set	Yes	1
AGAP000720[a]	Ig C2-set; Ig I-set; Ig V-set; Ig V-set, subgroup; Ig subtype 2	Yes	1
AGAP001633	Ig I-set; Ig V-set; Ig subtype 2	No	0
AGAP001662	Ig I-set; Ig V-set; Ig subtype 2	No	0
AGAP001892	Ig E-set	No	0
AGAP001894	Ig E-set	No	0
AGAP002336	Ig I-set; Ig V-set subgroup; Ig subtype 2	No	1
AGAP002802	Ig I-set; Ig V-set subgroup; Ig subtype 2	No	1
AGAP002848[a]	Ig E-set	Yes	0
AGAP003656	Ig MHC, conserved site; Ig I-set; Ig V-set; Ig subtype 2	No	0
AGAP004335	Ig E-set	Inc. seq.	0
AGAP005471	Ig I-set; Ig V-set Ig V-set subgroup; Ig subtype 2	No	0
AGAP005549	Ig MHC, conserved site	No	0
AGAP007562	Ig I-set; Ig V-set; Ig subtype 2	No	0
AGAP007563	Ig C1-set; Ig I-set; Ig V-set; Ig subtype 2	No	0
AGAP008408	Ig I-set; Ig subtype 2	No	1
AGAP008813	Ig I-set; Ig subtype	Inc. seq.	1
AGAP009515	Ig E-set	No	0
AGAP010428	Ig E-set	No	0
AGAP010821	Ig C2-set	Inc. seq.	0
AGAP010823[a]	Ig C2-set	Yes; Inc. seq.	1
AGAP010877	Ig E-set	Inc. seq.	0
AGAP010964	Ig Cl-set	Inc. seq.	0
AGAP011578[a]	Ig-like	Yes; Inc. seq.	0
AGAP011700	Ig I-set; Ig V-set; Ig subtype 2	No	0
AGAP011859	Glycoside hydrolase, family 2, Ig-like beta-sandwich	No	0
AGAP012168	Ig E-set	No	0
AGAP012343	Ig C2-set; Ig Cl-set; Ig I-set; Ig V-set; Ig subtype 2	Inc. seq.	1
AGAP013106[a]	Ig E-set	Yes	0

[a] Denotes proteins which are predicted to be extracellular. Transmembrane Domain (TMD). Ig, immunoglobulin; Inc. seq., incomplete sequence; MHC, major histocompatibility complex.

or surface-associated proteins. Members of the immunoglobulin superfamily play roles in cell−cell adhesion and recognition, function as cell-surface receptors, and in higher eukaryotes, are involved in the adaptive immune system.[54] Approximately 138 genes in the *An. gambiae* genome are predicted to contain a minimum of one immunoglobulin domain.[55] Of the Ig-like proteins identified in the DRM proteome, 45% contained I-set (intermediate, IPR013098) domains, which are found but not limited to several canonical cell adhesion and junction adhesion molecules in eukaryotes.[54] The precise function of the majority of these *Anopheles* proteins is unknown. However, genetic silencing by RNA interference demonstrated a role for a subset of these genes in controlling bacterial and parasitic infection. In particular, knock down of *IRD4* (AGAP003656) and *IRD6* (AGAP005471, resulted in an approximate 2-fold increase of *P. falciparum* oocysts compared to controls, suggesting that these genes play a role in restricting *Plasmodium* infection.[55] Both AGAP003656-PA and AGAP005471-PA were detected in the DRM fractions, and further examination of these immunoglobulin domain-containing proteins identified in DRMs may reveal a role for DRMs in mosquito immunity. Moreover, the identification of an immunoglobulin domain containing proteins as well as the protein products of previously characterized immune-responsive genes in the midgut DRM proteome suggests that the observed up-regulation in transcript levels for a subset of these "immune genes" 18−24 h post infectious blood feeding[29,30] may in fact represent an intrinsic midgut response to replenish the tissues apical epithelial surface architecture following blood feeding, and not necessarily a result of a direct response to the malaria parasite. For example, an interrogation of the available angaGEDU-CI: *An. gambiae* gene expression database (http://www.angaged.bio.uci.edu)[56] using accession numbers from our DRM proteome, representing proteins that contain either a leucine-rich domain (AGAP005744; AGAP006643), an immunoglobulin domain (AGAP000550; AGAP002848; AGAP012168) or adhesion/lectin-like domains (AGAP000341; AGAP006280; AGAP005404) underscore the possibility of expression discordance in transcript and protein presence in the midgut of sugar-fed and blood fed *An. gambiae* (data not shown). Therefore, we contend that caution must be taken since an observed upregulation of transcript during the first 3−24 h following blood feeding may not necessarily correspond to a commensurate expression of protein. Without empirical validation of protein presence in sugar-fed midguts, one cannot say that a protein is only present in blood fed midguts.

Glycosylation of DRM-Associated Proteins

The apical membrane of the midgut is heavily glycosylated and coated with a glycocalyx, an electron-dense layer rich in glycans,

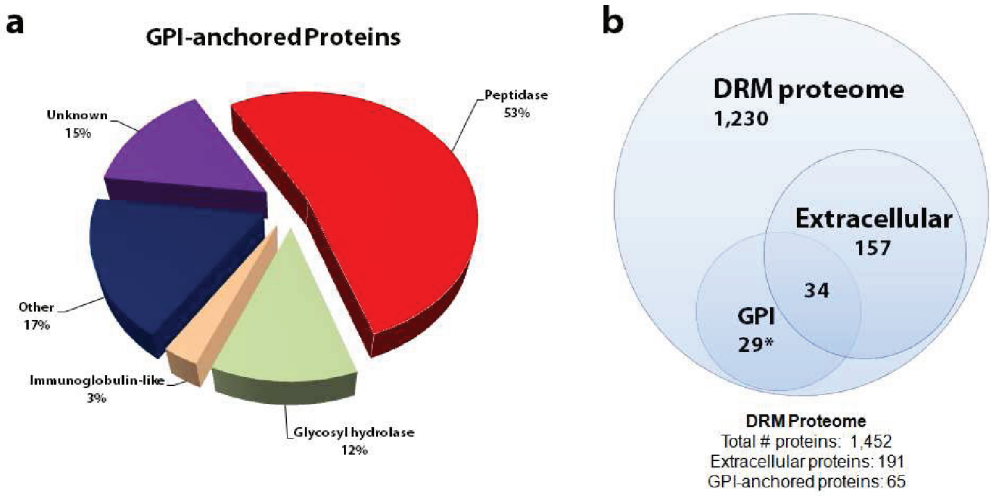

Figure 3. *An. gambiae* midgut brush border microvilli GPI-anchored subproteome. (a) PepArML identified 65 proteins from a combined search using Mascot, OMSSA, and X!Tandem at <1% FDR. Distribution of the identified GPI-anchored proteins ($N = 65$) into categories was based on function (see text and Table S5, Supporting Information, for details). (b) Venn diagram illustrating the common proteins that were identified in the GPI, extracellular DRM, and total DRM proteomes. *, two proteins, AGAP004944 and AGAP012745, that were identified in the GPI-anchored subproteome were not identified in the DRM proteome (<1%FDR).

which protects the midgut epithelial cells from the enzymatic processes involved with digestion. *O*-glycans have also been shown to be important mediators of ookinete attachment and invasion.[11,57] The amino acid sequences of all predicted extracellular DRM-associated proteins were analyzed for the presence of predicted glycosylation sites. A total of 121 proteins were predicted to have at least one *O*-linked glycosylation site and 145 proteins were predicted to have at least one *N*-linked glycosylation site (Table S2, Supporting Information). Jacalin binds to galactose and GalNAc residues and has previously been shown to competitively inhibit ookinete attachment to the midgut.[58] The GalNAc residues were also shown to be conserved between *Aedes* and *Anopheles* mosquitoes, and similarly involved in ookinete attachment.[11,59] A follow-up study used jacalin column chromatography and LC−MS/MS to identify the predominant heavily *O*-glycosylated midgut proteins that are recognized by this lectin on *An. gambiae*.[11] Of the five proteins identified in that study, four of them, AGAP004809 (AgAPN1), AGAP001881 (AgAPN3), and two glycosyl hydrolases, AGAP003995 (alpha-glucosidase) and AGAP012401, a previously described maltase-like protein (AgM1),[60] were detected in the DRM fractions indicating that *O*-glycosylated proteins are present in midgut DRMs.

GPI-Anchored Proteins Are Enriched in the DRM Fractions

Since the number of reagents available for confirming anopheline homologues of common DRM-associated proteins are limited, an orthogonal approach was taken to validate our bioinformatics approach as well as to confirm the technical validity of our DRM isolation approach. As GPI-anchored proteins are known to be enriched in DRMs,[6] we examined the GPI proteome of *An. gambiae* midgut brush border microvilli to confirm enrichment of GPI-anchored proteins in our DRM fractions. Sugar-fed midguts were used for three biological replicate BBMV preparations, which were subsequently treated with phosphatidylinositol-specific phospholipase C (PI-PLC), an enzyme known to specifically release GPI-anchored proteins from the membrane. From three biological replicate preparations, a PepArML search against VectorBase identified 76 proteins that were finally clustered to 65 proteins (Figure 3a and Table S4, Supporting Information). Of the 65 proteins identified in the GPI-anchored protein subproteome, 96.9% are also present in the DRM proteome (Figure 3b).

All GPI-anchored proteins contain both an N-terminal signal sequence and a C-terminal sequence, which is cleaved and eventually replaced with a GPI-anchor.[61] Of the 65 proteins, 39 had a predicted signal sequence, which is a requirement for the addition of a GPI anchor. Among these 39 proteins, five proteins were predicted to be nonsecreted intracellular contaminants based on sequence homology. Thus, based on the presence of a signal peptide and the removal of 5 intracellular proteins, we predict that 34 proteins in the GPI proteome are extracellular. Proteins detected in the GPI-anchored protein fraction that were predicted to be extracellular included: peptidases (52.9%), glycosyl hydrolases (11.7%), proteins in the unknown function (14.7%), proteins containing an immunoglobulin-like domain (2.9%), and proteins categorized as "other" (17.6%). Alkaline phosphatases have been previously reported to be surface-associated and enriched in BBMVs from aedine and anopheline larvae but were, in general, regarded as inappropriate markers for the midgut surface.[42,62] However, given that AGAP006400 and AGAP011302 were identified in the GPI-anchored midgut subproteome (Table S4, Supporting Information), these specific species of alkaline phosphatase may be appropriate as midgut surface marker. Also, it has been shown that PI-PLC treatment of BBMVs releases both the 125 kDa isoform of the GPI-anchored AgAPN1 as well as a truncated ~60 kDa isoform.[11] AgAPN1 was detected in our GPI-anchored subproteome confirming this previous finding and also provides a known GPI-anchored marker to confirm the isolation of GPI-anchored proteins in our subproteome. Taken together, these data demonstrate that our DRM fractions are enriched in GPI-anchored proteins, which are common markers of DRMs, thus providing additional supporting evidence that our midgut DRM fractions do indeed contain DRMs.

Ookinete-Interacting Proteins Partition into the DRM Fractions

The process of ookinete invasion of the midgut epithelium is likely to involve a hierarchy of multiple protein−glycan and

protein−protein interactions, ranging from attachment to the midgut surface to penetration and crossing of the midgut apical plasma membrane.[2] Experimental evidence from previous studies indicated that AgAPN1, ANXB9, ANXB10B, ANXB10C, CpbAg1, and SCRBQ2 mediate the ookinete invasion process (Table 1). Given our hypothesized role of DRMs in partitioning important midgut ligands at the site of ookinete invasion, a reasonable expectation would be the confirmatory presence of these six proteins in our DRM fraction, since partitioning requires association of these proteins to mobile rafts. Our analyses of the DRM fractions revealed that five out of six of these proteins, AgAPN1, ANXB9, ANXB10B, CpbAg1, and SCRBQ2, are indeed DRM-associated (Table 1), providing inferred but plausible support for the role for DRM partitioning of proteins utilized by ookinetes to transverse the midgut epithelium. ANXB10C was the only known ookinete interacting protein not detected in any of our DRM preparations. Two of the known ookinete-interacting proteins, AgAPN1 and CpbAg1, are peptidases. Peptidases comprised 27.7% and 52.9% of the total extracellular DRM proteins and of the extracellular subset of identified GPI-anchored proteins, respectively, indicating that peptidases are highly abundant proteins on the midgut surface. From a pathogen's perspective, selecting highly abundant proteins on the host surface would facilitate host cell recognition, attachment, and invasion. Fifty-two other DRM-associated peptidases were predicted to be extracellular and further characterization of these peptidases may lead to the characterization of other midgut proteins that mediate ookinete invasion.

It can be argued that since our DRM preparations used sugar-fed midguts, it may not completely reflect the DRM proteome in which the ookinete interacts with *in vivo*. Upon ingestion of a blood meal, the PM separates the blood meal bolus from the apical microvillar surface. Both the formation of the PM, the distension of the midgut after a blood meal, as well as the presence of blood in the lumen of the midgut may influence protein expression and protein residency in DRMs. We used sugar-fed midguts in this study for a number of reasons. First, doing so facilitated the identification by mass spectrometry of low abundance *Anopheles* midgut DRM-associated proteins that would have otherwise been difficult to achieve due to the gross quantities of blood and serum proteins contaminating our DRM preparations. Second, although several microarray studies have shown differential expression of the *Anopheles* midgut transcriptome in response to *Plasmodium* invasion,[29,30] these genes appear to be primarily involved in immunity and are upregulated after the ookinete has invaded the midgut epithelium. Thus, these changes in gene expression may have little effect on the initial ookinete interactions with the midgut surface. Most importantly, to our knowledge, experimental validation by Western blotting of the assumed 1:1 concordance of transcript abundance with protein translation/presence for these immune-responsive genes is largely missing. In fact, this is the first report detecting the presence of proteins from the immunoglobulin-like domain family of proteins in sugar-fed midguts, which further supports this assertion. Third, many apical membrane proteins present on the surface of blood-fed midguts are already surface-associated in sugar-fed midguts. For example, AgAPN1[11] and AgMUC-1,[12] a midgut surface-associated mucin-like protein, as well as critical *O*-linked glycans on midgut surface glycoproteins[2,57,59] have been shown to be surface associated in sugar-fed and blood-fed midguts by immunofluorescence microscopy. Additionally, in our proteomic analysis of DRMs from sugar-fed midguts, we were able to detect the presence of five known ookinete-interacting proteins. While it can be argued that DRM-residency of proteins can change across time and space, especially postblood feeding, our data suggest that at least prior to acquiring an infectious bloodmeal, many ookinete-interacting proteins are already present in DRMs before the ingestion of an infected blood meal. Therefore, we believe that the sugar-fed midgut DRM proteome has physiological significance in terms of ookinete−midgut interactions but still recognize that our approach may not necessarily capture the complete proteomic landscape 18−24 h postblood feeding.

A Model of Ookinete Interaction with Mosquito Midgut Host DRM (Lipid Raft) Proteins

Throughout nature, DRMs are exploited by pathogens as entry points into host cells. In this study, we propose that *Plasmodium* ookinetes interact with midgut DRMs to cross the midgut epithelium. Also, we report the first description of the DRM proteome of *An. gambiae* midguts in which we identified 1452 proteins. Furthermore, examination of the GPI proteome and immunoblots probed with specific antibodies demonstrated that our DRM fractions contain GPI-anchored proteins, such as AgAPN1. Analysis of the proteins identified in the DRM fractions revealed that five known ookinete-interacting proteins were present. These results provided the basis for a proposed model in which ookinetes interact with a subset of midgut DRM-associated proteins to transverse the midgut epithelium.

Given our mass spectrometry evidence suggesting the presence of known parasite "interacting" proteins in midgut DRMs, we propose a working model in which interactions between a subset of midgut DRM-associated proteins and the ookinete facilitate the invasion process (Figure 4). Lipid rafts allow for the partitioning of multiple ookinete-interacting proteins into discrete locations on the midgut surface, enhancing multivalent interactions between the ookinete and the midgut. Multivalent interactions have been suggested to be a conserved process for strengthening single, protein−protein, or protein−glycan interactions for several vector-borne pathogens, including *Plasmodium*.[2] In one example, a complex set of events that require lipid raft integrity, lateral mobility, and partitioning on midgut surfaces has been shown to be essential for Cry1a toxin insertion and pore formation in *Heliothis virescens* and *Manducta sexta*.[63]

From our proteomic analysis, we know that, long before the ookinete contacts the midgut surface, many of the DRM-associated proteins utilized by the ookinete already exist in rafts (Figure 4a). This is evident by the fact that the ookinete-interacting proteins (AgAPN1, ANXB9, ANXB10B, CpbAg1, and SCRBQ2) were detected in our DRM preparations, which used sugar-fed midguts from mosquitoes that had no previous blood meal or exposure to *Plasmodium* parasites.

Previous studies have shown that ookinetes glide along the midgut surface toward the junctions between cells before invasion occurs.[64] After initial contact is made with the midgut microvillar surface, we propose that the ookinete engages a subset of specific rafts following one of two (or a combination of) different mechanisms. The first possibility (1) is that the ookinete interacts with single or multiple rafts already at the site of invasion (depicted by the red arrowhead, Figure 4b). Here, the fusion of rafts may not be necessary for ookinete invasion as the partitioning of host receptors in individual rafts may already be of sufficient density to promote multivalent interactions.

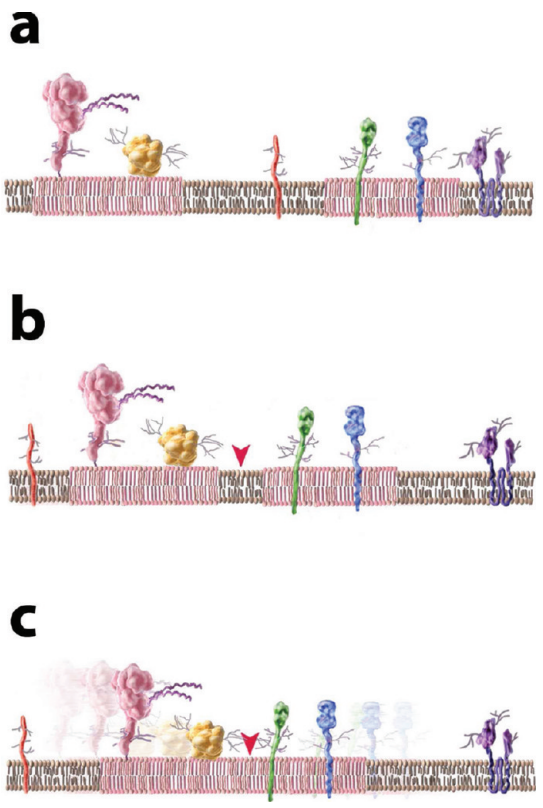

Figure 4. Model illustrating how partitioned midgut DRM-associated proteins can be utilized by *Plasmodium* ookinetes to adhere to the midgut epithelium. (a) Ookinete-interacting proteins exist in DRMs (rafts) before the ookinete makes contact with the midgut surface. (b) Potential model of ookinetes utilizing individual DRMs (rafts) containing ookinete-interacting proteins at the site of invasion to invade the midgut epithelium. (c) Potential model of DRMs (rafts) fusing to form a large platform containing ookinete-interacting proteins at the site of invasion, which would facilitate ookinete invasion of the midgut epithelium. Red arrowhead, hypothetical site of ookinete interaction along the midgut plasmalemma.

The second model (2) is that the ookinete induces multiple small rafts to mobilize and fuse forming a large platform of partitioned ookinete-interacting proteins at the site of invasion on the midgut surface (Figure 4c). Both hypotheses include the central theme of ookinetes utilizing rafts as a means of accessing partitioned host receptors in a specific region of the midgut apical membrane. Unfortunately, it is difficult to test whether or not raft fusion is involved in the invasion process. Currently, a polarized *Anopheles* midgut epithelial cell line does not exist; thus, our experimental design is limited to studies involving whole organisms. Development of a midgut epithelial cell line would aid in elucidating the precise molecular interactions between midgut DRM-associated proteins and the ookinete and in determining if raft fusion occurs in the invasion process.

Lastly, we cannot exclude the possibility that proteins that are not associated with DRMs may also be involved in the invasion process. ANXB10C along with several other non-DRM associated proteins may in fact be present at the site of invasion. It is possible that accumulation of the DRM-associated proteins in close proximity to, if not in complex with, these non-DRM ligands, facilitates the ookinete invasion process. Unfortunately, to date a comprehensive analysis of a whole host of apical microvilli glycoproteins has not yet been achieved.

Plasmodium Subversion of Host Red Cell DRMs

While this study is the first to propose an interaction between *Plasmodium* ookinetes with midgut DRMs, previous studies have suggested that *Plasmodium* merozoites may engage host DRMs to enter erythrocytes.[65,66] During invasion, the erythrocyte plasma membrane indents forming a vacuole around the invading merozoite known as the parasitophorous vacuole membrane (PVM), where the parasite will reside for the duration of its intraerythrocytic cycle. Erythrocyte DRM-associated proteins CD55, CD59, Duffy, flotillin-1, and flotillin-2 are detected in the PVM but glycophorin A, glycophorin C, CD47, and ankyrin, which are not present in DRMs, are excluded from the PVM.[65] Since the PVM originates from the point of merozoite entry, the presence of erythrocyte DRM-associated proteins in the PVM imply that DRMs are utilized by the merozoite at some point during the invasion process. Moreover, some erythrocyte DRM-associated proteins are excluded from the PVM suggesting that merozoites interact only with a particular subset of rafts on the surface of the erythrocyte.[65] The biological relevance of lipid raft involvement in parasite invasion is further supported by the observation that treatment of uninfected erythrocytes with lidocaine, which disrupts lipid rafts, inhibits merozoite invasion of these erythrocytes.[66] Although ookinetes do not form a PVM during invasion, both merozoite invasion of erythrocytes and ookinete invasion of the midgut epithelium appear to be mechanistically similar in that host DRM-associated proteins are involved in mediating the invasion process.

In conclusion, our proteomic analysis of *An. gambiae* midgut epithelial surface DRMs suggests that *Plasmodium* ookinetes may interact with midgut proteins that are partitioned in membrane microdomains. These findings advance significantly our current understanding of the mosquito midgut microvillar surface and open new avenues in the study of ookinete invasion of the midgut, an essential step for *Plasmodium* transmission through the mosquito. Uncharacterized DRM-associated proteins identified in this study may prove to be necessary for efficient midgut invasion by ookinetes. A thorough interrogation of the results is needed to screen for important targets of *Plasmodium* interaction that, in turn, may lead to the development of novel mosquito-based transmission-blocking vaccines.

■ ASSOCIATED CONTENT

Supporting Information

Figure S1. Lipid Raft Fractions IV−VI. SDS-PAGE SYPRO Ruby stained 4−12% Invitrogen gel of fractions 4, 5, 6, 7, 8, 9, 10,11, pellet, and a sample of the midgut lysate before separation on a sucrose gradient. Approximately 2 μg of protein was loaded per well. Lane a, Mark12 ladder (Invitrogen); Lane b, fraction 4; Lane c, fraction 5; Lane d, fraction 6; Lane e, fraction 7; Lane f, fraction 8; Lane g, fraction 9; Lane h, fraction 10; Lane i, fraction 11; Lane j, pellet; Lane k, total midgut lysate before separation on a sucrose gradient. The DRM fractions are highlighted by an asterisk. This representative gel from all three biological replicate fractionations was imaged using a 9210 Typhoon imager (PMT of 500 V and 25 μM resolution). This material is available free of charge via the Internet at http://pubs.acs.org.

■ AUTHOR INFORMATION

Corresponding Author

*Rhoel R. Dinglasan, rdinglas@jhsph.edu. Phone +1-410-614-4839. Fax +1-410-955-0105.

■ ACKNOWLEDGMENT

We thank Derrick Mathias, Rebecca Pastrana-Mena, and Jennifer Armistead for critical review of the manuscript and Nathan J. Edwards for additional bioinformatics and computing support. This work was supported in part by grants K22AI077707-02 and R01AI082587-01 to R.R.D and fellowship support from 5T32AI007417-17 for L.A.P. from the NIAID, NIH; grant HHSN268201000032C (N01−HV-00240) from NHLBI to D.R.G., as well as seed funding from the Bloomberg Family Foundation to R.R.D.

■ ABBREVIATIONS

AHC, agglomerative hierarchical clustering; BBMV, brush border microvilli vesicles; DRM, detergent resistant membranes; DTT, dithiothreitol; FDR, false discovery rate; GPI, glycosylphosphotidyl inositol; LC, liquid chromatography; PI-PLC, phosphotidylinositol-specific phospholipase; PM, peritrophic matrix; PVM, parasitophorous vacuole membrane; TBV, transmission blocking vaccine; TFA, trifluoroacetic acid

■ REFERENCES

(1) Dinglasan, R. R.; Jacobs-Lorena, M. Flipping the paradigm on malaria transmission-blocking vaccines. *Trends Parasitol.* **2008**, *24* (28), 364–370.

(2) Dinglasan, R. R.; Jacobs-Lorena, M. Insight into a conserved lifestyle: protein-carbohydrate adhesion strategies of vector-borne pathogens. *Infect. Immun.* **2005**, *73* (12), 7797–7807.

(3) Lavazec, C.; Bourgouin, C. Mosquito-based transmission-blocking vaccines for interrupting Plasmodium development. *Microbes Infect.* **2008**, *10* (8), 845–849.

(4) Harris, T. J.; Siu, C. H. Reciprocal raft-receptor interactions and the assembly of adhesion complexes. *BioEssays: News Rev. Mol., Cell. Dev. Biol.* **2002**, *24* (11), 996–1003.

(5) Simons, K.; Gerl, M. J. Revitalizing membrane rafts: new tools and insights. *Nat. Rev. Mol. Cell Biol.* **2010**, *11* (10), 688–99.

(6) Simons, K.; Ikonen, E. Functional rafts in cell membranes. *Nature* **1997**, *387* (6633), 569–572.

(7) London, E.; Brown, D. A. Insolubility of lipids in triton X-100: Physical origin and relationship to sphingolipid/cholesterol membrane domains (rafts). *Biochim. Biophys. Acta* **2000**, *1508* (1−2), 182–195.

(8) Foster, L. J.; De Hoog, C. L.; Mann, M. Unbiased quantitative proteomics of lipid rafts reveals high specificity for signaling factors. *Proc. Natl. Acad. Sci. U.S.A.* **2003**, *100* (10), 5813–5818.

(9) Riethmuller, J.; Riehle, A.; Grassme, H.; Gulbins, E. Membrane rafts in host-pathogen interactions. *Biochim. Biophys. Acta* **2006**, *1758* (12), 2139–2147.

(10) Mittal, K.; Welter, B. H.; Temesvari, L. A. Entamoeba histolytica: lipid rafts are involved in adhesion of trophozoites to host extracellular matrix components. *Exp. Parasitol.* **2008**, *120* (2), 127–134.

(11) Dinglasan, R. R.; Kalume, D. E.; Kanzok, S. M.; Ghosh, A. K.; Muratova, O.; Pandey, A.; Jacobs-Lorena, M. Disruption of Plasmodium falciparum development by antibodies against a conserved mosquito midgut antigen. *Proc. Natl. Acad. Sci. U.S.A.* **2007**, *104* (33), 13461–13466.

(12) Kotsyfakis, M.; Ehret-Sabatier, L.; Siden-Kiamos, I.; Mendoza, J.; Sinden, R. E.; Louis, C. Plasmodium berghei ookinetes bind to Anopheles gambiae and Drosophila melanogaster annexins. *Mol. Microbiol.* **2005**, *57* (1), 171–179.

(13) Lavazec, C.; Bonnet, S.; Thiery, I.; Boisson, B.; Bourgouin, C. cpbAg1 encodes an active carboxypeptidase B expressed in the midgut of Anopheles gambiae. *Insect Mol. Biol.* **2005**, *14* (2), 163–174.

(14) Gonzalez-Lazaro, M.; Dinglasan, R. R.; Hernandez-Hernandez, F.; de, L.; Rodriguez, M. H.; Laclaustra, M.; Jacobs-Lorena, M.; Florez-Romo, L. Anopheles gambiae croquemort SCRBQ2, expression profile in the mosquito and its potential interaction with the malaria parasite Plasmodium berghei. *Insect Biochem. Mol. Biol.* **2009**, *39* (5−6), 395–402.

(15) Rodríguez, M. C.; Martínez-Barnetche, J.; Alvarado-Delgado, A.; Batista, C.; Argotte-Ramos, R. S.; Hernández-Martínez, S.; González Cerón, L.; Torres, J. A.; Margos, G.; Rodríguez, M. H. The surface protein Pvs25 of Plasmodium vivax ookinetes interacts with calreticulin on the midgut apical surface of the malaria vector Anopheles albimanus. *Mol. Biochem. Parasitol.* **2007**, *153* (2), 167–177.

(16) King, J. Y.; Ferrara, R.; Tabibiazar, R.; Spin, J. M.; Chen, M. M.; Kuchinsky, A.; Vailaya, A.; Kincaid, R.; Tsalenko, A.; Deng, D. X.; Connolly, A.; Zhang, P.; Yang, E.; Watt, C.; Yakhini, Z.; Ben-Dor, A; Adler, A.; Bruhn, L.; Tsao, P.; Quertermous, T.; Ashley, E. A. Pathway analysis of coronary atherosclerosis. *Physiol. Genomics* **2005**, *23* (1), 103–118.

(17) Perkins, D. N.; Pappin, D. J.; Creasy, D. M.; Cottrell, J. S. Probability-based protein identification by searching sequence databases using mass spectrometry data. *Electrophoresis* **1999**, *20*, 3551–3567.

(18) Geer, L. Y.; Markey, S. P.; Kowalak, J. A.; Wagner, L.; Xu, M.; Maynard, D. M.; Yang, X.; Shi, W.; Bryant, S. H. Open mass spectrometry search algorithm. *J. Proteome Res.* **2004**, *3* (5), 958–964.

(19) Craig, R.; Beavis, R. C. Tandem: matching proteins with tandem mass spectra. *Bioinformatics* **2004**, *20* (9), 1466–1467.

(20) Edwards, N.; Wu, X.; Tseng, C. W. An unsupervised, Model-Free, Machine-Learning Combiner for Peptide Identifications from Tandem Mass Spectra. *Clin. Proteomics* **2009**, *5* (1), 23–36.

(21) Hall, M.; Frank, E.; Holmes, G.; Pfahringer, B.; Reutemann, P.; Witten, I. H. The WEKA Data Mining Software: An Update. *SIGKDD Explorations Newslett.* **2009**, *11*, 1.

(22) Ubaida Mohien, C.; Hartler, J.; Breitwieser, F.; Rix, U.; Rix, L. R.; Winter, G. E.; Thallinger, G. G.; Bennett, K. L.; Superti-Furga, G.; Trajanoski, Z.; Colinge, J. MASPECTRAS 2: An integration and analysis platform for proteomic data. *Proteomics* **2010**, *10* (14), 2719–2722.

(23) Jones, A. R.; Siepen, J. A.; Hubbard, S. J.; Paton, N. W. Improving sensitivity in proteome studies by analysis of false discovery rates for multiple search engines. *Proteomics* **2009**, *9* (5), 1220–1229.

(24) Dagda, R. K.; Sultana, T.; Lyons-Weiler, J. Evaluation of the Consensus of Four Peptide Identification Algorithms for Tandem Mass Spectrometry Based Proteomics. *J. Proteomics Bioinform.* **2010**, *3*, 9–47.

(25) Kapp, E. A.; Schütz, F.; Connolly, L. M.; Chakel, J. A.; Meza, J. E.; Miller, C. A.; Fenyo, D.; Eng, J. K.; Adkins, J. N.; Omenn, G. S.; Simpson, R. J. An evaluation, comparison, and accurate benchmarking of several publicly available MS/MS search algorithms: sensitivity and specificity analysis. *Proteomics* **2005**, *5* (13), 3475–3490.

(26) Oda, H.; Uemura, T.; Harada, Y.; Iwai, Y.; Takeichi, M. A Drosophila homolog of cadherin associated with armadillo and essential for embryonic cell-cell adhesion. *Dev. Biol.* **1994**, *165* (2), 716–726.

(27) Tepass, U.; Gruszynski-DeFeo, E.; Haag, T. A.; Omatyar, L.; Torok, T.; Hartenstein, V. Shotgun encodes Drosophila E-cadherin and is preferentially required during cell rearrangement in the neurectoderm and other morphogenetically active epithelia. *Genes Dev.* **1996**, *10* (6), 672–685.

(28) Devenport, M.; Fujioka, H.; Donnelly-Doman, M.; Shen, Z.; Jacobs-Lorena, M. Storage and secretion of Ag-Aper14, a novel peritrophic matrix protein, and Ag-Muc1 from the mosquito Anopheles gambiae. *Cell Tissue Res.* **2005**, *320* (1), 175–185.

(29) Vlachou, D.; Schlegelmilch, T.; Christophides, G. K.; Kafatos, F. C. Functional genomic analysis of midgut epithelial responses in Anopheles during Plasmodium invasion. *Curr. Biol.* **2005**, *15* (13), 1185–1195.

(30) Dong, Y.; Aguilar, R.; Xi, Z.; Warr, E.; Mongin, E.; Dimopoulos, G. Anopheles gambiae immune responses to human and rodent Plasmodium parasite species. *PLoS Pathog.* **2006**, *2* (6), e52.

(31) Zdobnov, E. M.; von Mering, C.; Letunic, I.; Torrents, D.; Suyama, M.; Copley, R. R.; Christophides, G. K.; Thomasova, D.; Holt, R. A.; Subramanian, G. M.; Mueller, H. M.; Dimopoulos, G.; Law, J. H.; Wells, M. A.; Birney, E.; Charlab, R.; Halpern, A. L.; Kokoza, E.; Kraft, C. L.; Lai, Z.; Lewis, S.; Louis, C.; Barillas-Mury, C.; Nusskern, D.; Rubin, G. M.; Salzberg, S. L.; Sutton, G. G.; Topalis, P.; Wides, R.;

Wincker, P.; Yandell, M.; Collins, F. H.; Ribeiro, J.; Gelbart, W. M.; Kafatos, F. C.; Bork, P. Comparative genome and proteome analysis of Anopheles gambiae and Drosophila melanogaster. *Science* **2002**, *298* (5591), 149–159.

(32) Behmer, S. T.; Nes, W. D. Insect sterol nutrition and physiology: A global overview. In *Advances in insect physiology*; Simpson, S. J., Ed.; Academic Press: New York, 2003l pp 1−72.

(33) Svoboda, J. A.; Thompson, M. J.; Herbert, E. W.; Shortino, T. J.; Szczepanik-Vanleeuwen, P. A. Utilization and metabolism of dietary sterols in the honey bee and the yellow fever mosquito. *Lipids* **1982**, *17* (3), 220–225.

(34) Krebs, K. C.; Lan, Q. Isolation and expression of a sterol carrier protein-2 gene from the yellow fever mosquito, Aedes aegypti. *Insect Mol. Biol.* **2003**, *12* (1), 51–60.

(35) Lan, Q.; Massey, R. J. Subcellular localization of the mosquito sterol carrier protein-2 and sterol carrier protein-x. *J. Lipid Res.* **2004**, *45* (8), 1468–1474.

(36) Giocondi, M. C.; Vié, V.; Lesniewska, E.; Goudonnet, J. P.; Le Grimellec, C. In situ imaging of detergent-resistant membranes by atomic force microscopy. *J. Struct. Biol.* **2000**, *131* (1), 38–43.

(37) Forcella, M.; Berra, E.; Giacchini, R.; Parenti, P. Leucine transport in brush bordermembrane vesicles from freshwater insect larvae. *Arch. Insect Biochem. Physiol.* **2006**, *63* (3), 110–122.

(38) Popova-Butler, A.; Dean, D. H. Proteomic analysis of the mosquito Aedes aegypti midgut brush border membrane vesicles. *J. Insect Physiol.* **2009**, *55* (3), 264–272.

(39) Houk, E. J.; Arcus, Y. M.; Hardy, J. L. Isolation and characterization of brush border fragments from mosquito mesenterons. *Arch. Insect Biochem. Physiol.* **1986**, *3* (2), 135–146.

(40) Braccia, A.; Villani, M.; Immerdal, L.; Niels-Christiansen, L. L.; Nystrøm, B. T.; Hansen, G. H.; Danielsen, E. M. Microvillar membrane microdomains exist at physiological temperature. Role of galectin-4 as lipid raft stabilizer revealed by "superrafts. *J. Biol. Chem.* **2003**, *278* (18), 15679–15684.

(41) Babiychuk, E. B.; Draeger, A. Annexins in cell membrane dynamics. Ca (2+)-regulated association of lipid microdomains. *J. Cell Biol.* **2000**, *150* (5), 1113–1124.

(42) Danielsen, E. M. Involvement of detergent-insoluble complexes in the intracellular transport of intestinal brush border enzymes. *Biochemistry* **1995**, *34* (5), 1596–1605.

(43) Assossou, O.; Besson, F.; Rouault, J. P.; Persat, F.; Brisson, C.; Duret, L.; Ferrandiz, J.; Mayencon, M.; Peyron, F.; Picot, S. Subcellular localization of 14−3-3 proteins in Toxoplasma gondii tachyzoites and evidence for a lipid raft-associated form. *FEMS Microbiol. Lett.* **2003**, *224* (2), 161–168.

(44) Hughes, R. C. Secretion of the galectin family of mammalian carbohydrate-binding proteins. *Biochim. Biophys. Acta* **1999**, *1473* (1), 172–185.

(45) Christmas, P.; Callaway, J.; Fallon, J.; Jones, J.; Haigler, H. T. Selective secretion of annexin 1, a protein without a signal sequence, by the human prostate gland. *J. Biol. Chem.* **1991**, *266* (4), 2499–2507.

(46) Alberti-Segui, C.; Morales, A. J.; Xing, H.; Kessler, M. M.; Willins, D. A.; Weinstock, K. G.; Cottarel, G.; Fechtel, K.; Rogers, B. Identification of pote ntial cell-surface proteins in Candida albicans and investigation of the role of a putative cell-surface glycosidase in adhesion and virulence. *Yeast* **2004**, *21* (4), 285–302.

(47) Billingsley, P. F.; Hecker, H. Blood digestion in the mosquito, Anopheles stephensi Liston (Diptera: Culicidae): activity and distribution of trypsin, aminopeptidase, and alpha-glucosidase in the midgut. *J. Med. Entomol.* **1991**, *28* (6), 865–871.

(48) Suwanchaichinda, C.; Kanost, M. R. The serpin gene family in Anopheles gambiae. *Gene* **2009**, *442* (1−2), 47–54.

(49) Dinglasan, R. R.; Devenport, M.; Florens, L.; Johnson, J. R.; McHugh, C. A.; Donnelly-Doman, M.; Carruci, D. J.; Yates, J. R.; Jacobs-Lorena, M. The Anopheles gambiae adult midgut peritrophic matrix proteome. *Insect Biochem. Mol. Biol.* **2009**, *39* (2), 125–134.

(50) Devenport, M.; Fujioka, H.; Donnelly-Doman, M.; Shen, Z.; Jacobs-Lorena, M. Storage and secretion of the peritrophic matrix protein ag-Aper1 and trypsin in the midgut of Anopheles gambiae. *Insect Mol. Biol.* **2004**, *13* (4), 349–358.

(51) Chasserot-Golaz, S.; Vitale, N.; Umbrecht-Jenck, E.; Knight, D.; Gerke, V.; Bader, M. F. Annexin 2 promotes the formation of lipid microdomains required for calcium-regulated exocytosis of dense-core vesicles. *Mol. Biol. Cell* **2005**, *16* (3), 1108–1119.

(52) Hynes, R. O. Integrins: Bidirectional, allosteric signaling machines. *Cell* **2002**, *110* (6), 673–687.

(53) Conforti, G.; Dominguez-Jimenez, C.; Zanetti, A; Gimbrone, M. A., Jr; Cremona, O.; Marchisio, P. C.; Dejana, E. Human endothelial cells express integrin receptors on the lumenal aspect of their membrane. *Blood* **1992**, *80* (2), 437–446.

(54) Aricescu, A. R.; Jones, E. Y. Immunoglobulin superfamily cell adhesion molecules: Zippers and signals. *Curr. Opin. Cell Biol.* **2007**, *19* (5), 543–550.

(55) Garver, L. S.; Xi, Z.; Dimopoulos, G. Immunoglobulin superfamily members play an important role in the mosquito immune system. *Dev. Comp. Immunol.* **2008**, *32* (5), 519–531.

(56) Dissanayake, S. N.; Marinotti, O.; Ribeiro, J. M.; James, A. A. angaGEDUCI: Anopheles gambiae gene expression database with integrated comparative algorithms for identifying conserved DNA motifs in promoter sequences. *BMC Genomics* **2006**, *7* (1), 116.

(57) Zieler, H.; Nawrocki, J. P.; Shahabuddin, M. Plasmodium gallinaceum ookinetes adhere specifically to the midgut epithelium of Aedes aegypti by interaction with a carbohydrate ligand. *J. Exp. Biol.* **1999**, *202* (Pt 5), 485–495.

(58) Zieler, H.; Garon, C. F.; Fischer, E. R.; Shahabuddin, M. A tubular network associated with the brush-border surface of the Aedes aegypti midgut: implications for pathogen transmission by mosquitoes. *J. Exp. Biol.* **2000**, *203* (Pt 10), 1599–1611.

(59) Dinglasan, R. R.; Fields, I.; Shahabuddin, M.; Azad, A. F.; Sacci, J. B. Monoclonal antibody MG96 completely blocks Plasmodium yoelii development in Anopheles stephensi. *Infect. Immun.* **2003**, *71* (12), 6995–7001.

(60) Zheng, L.; Whang, L. H.; Kumar, V.; Kafatos, F. C. Two genes encoding midgut-specific maltase-like polypeptides from Anopheles gambiae. *Exp. Parasitol.* **1995**, *81* (3), 272–283.

(61) Schonbachler, M.; Horvath, A.; Fassler, J.; Riezman, H. The yeast spt14 gene is homologous to the human PIG-A gene and is required for GPI-anchor synthesis. *EMBO J.* **1995**, *14* (8), 1637–1645.

(62) Abdul-Rauf, M.; Ellar, D. J. Isolation and characterization of brush border membrane vesicles from whole Aedes aegypti larvae. *J. Invertebr. Pathol.* **1999**, *73* (1), 45–51.

(63) Zhuang, M.; Oltean, D. I.; Gomez, I.; Pullikuth, A. K.; Soberon, M.; Bravo, A.; Gill, S. S. Heliothis virescens and Manduca sexta lipid rafts are involved in Cry1a toxin binding to the midgut epithelium and subsequent pore formation. *J. Biol. Chem.* **2002**, *277* (16), 13863–13872.

(64) Zieler, H.; Dvorak, J. A. Invasion in vitro of mosquito midgut cells by the malaria parasite proceeds by a conserved mechanism and results in death of the invaded midgut cells. *Proc. Natl. Acad. Sci. U.S.A.* **2000**, *97* (21), 11516–11521.

(65) Murphy, S. C.; Samuel, B. U.; Harrison, T.; Speicher, K. D.; Speicher, D. W.; Reid, M. E.; Prohaska, R.; Low, P. S.; Tanner, M. J.; Mohandas, N.; Haldar, K. Erythrocyte detergent-resistant membrane proteins: Their characterization and selective uptake during malarial infection. *Blood* **2004**, *103* (5), 1920–1928.

(66) Koshino, I.; Takakuwa, Y. Disruption of lipid rafts by lidocaine inhibits erythrocyte invasion by Plasmodium falciparum. *Exp. Parasitol.* **2009**, *123* (4), 381–383.